

The Anatomical Significance of the Patent Foramen Ovale by Real-time 3D TEE in Cryptogenic Stroke and Migraine

Li Wang¹, Haibo Sun², and Han Shen³

¹First Affiliated Hospital of Soochow University Department of Cardiology

²HYGEIA Su Zhou Yong Ding Hospital

³First Affiliated Hospital of Soochow University

September 02, 2024

Abstract

Abstract: Background: The transesophageal echocardiogram (TEE) is the standard imaging modality for confirming the presence or absence of patent foramen ovale. There is a causal association between PFO and unexplained stroke. It seems that 3D-TEE can present a high-risk PFO morphological feature, which seems to show more than just being easier to open. Methods: In total 134 consecutive patients with cryptogenic stroke or migraine who had suspected PFO and underwent c-TCD, TTE, and c-TEE were included in this study. TEE confirmed the PFO. The right-to-left shunt (RLS) grade of PFO at rest and abdominal compression Valsalva maneuver was detected by c-TEE. Results: The long diameter of FO (1.74 ± 0.3 vs. 1.60 ± 0.4 , $P=0.039$), the short diameter of FO (1.12 ± 0.3 vs. 1.00 ± 0.3 , $P=0.036$), perimeter of FO (4.62 ± 0.7 vs. 4.22 ± 1.0 , $P=0.026$) and area (1.80 ± 0.8 vs. 1.35 ± 0.8 , $P=0.05$) of the FO were significantly larger in the larger RLS group. The cut-off value calculated by ROC for the diagnosis of high-risk PFO was that the length of the PFO tunnel was 12 mm and Left funnellform combined with multiple exits of left atrial (sensitivity was 92%, specificity was 90%). Conclusions: A larger oval fossa can be more easily activated and cause a large right-to-left shunt. The left funnellform, a longer length of the PFO tunnel, and multiple exits of the tunnel of LA increase the risk of CS in anatomical of PFO respect. TEE can precisely visualize the specific morphological characteristics of PFO. These features on TEE have a strong correlation with CS.

The Anatomical Significance of the Patent Foramen Ovale by Real-time 3D TEE in Cryptogenic Stroke and Migraine

Li Wang¹, Haibo Sun³, Han Shen^{#2}

1 Department of Cardiology, The First Affiliated Hospital of Soochow University, Suzhou, China.

2 Department of Cardiovascular Surgery, The First Affiliated Hospital of Soochow University, Suzhou, China.

3. Department of Ultrasound, HYGEIA Su Zhou Yong Ding Hospital.

^{#2}.Correspondence to: Han Shen, MD, Department of Cardiovascular Surgery, The First Affiliated Hospital of Soochow University, 899 Pinghai Road, Gusu District, Suzhou, China. Email: shenhangongyong@126.com

Abstract:

Background:

The transesophageal echocardiogram (TEE) is the standard imaging modality for confirming the presence or absence of patent foramen ovale. PFO is a flap valve depending on the pressure change between the left and right atrium, which can help determine whether to open. 3D-TEE was shown to optimize the visualization of

PFO. There is a causal association between PFO and unexplained stroke. It seems that 3D-TEE can present a high-risk PFO morphological feature, which seems to show more than just being easier to open.

Methods: In total 134 consecutive patients with cryptogenic stroke or migraine who had suspected PFO and underwent c-TCD, TTE, and c-TEE were included in this study. TEE confirmed the PFO. The right-to-left shunt (RLS) grade of PFO at rest and abdominal compression Valsalva maneuver was detected by c-TEE.

Results:

The long diameter of FO (1.74 ± 0.3 vs. 1.60 ± 0.4 , $P=0.039$), the short diameter of FO (1.12 ± 0.3 vs. 1.00 ± 0.3 , $P=0.036$), perimeter of FO (4.62 ± 0.7 vs. 4.22 ± 1.0 , $P=0.026$) and area (1.80 ± 0.8 vs. 1.35 ± 0.8 , $P=0.05$) of the FO were significantly larger in the larger RLS group. In group of CS, a larger proportion of Eustachian valve or a Chiari's network (14.3% vs. 3.5%, $P=0.036$), a larger proportion of in the left funnelform (55.1% vs. 16.3% $P<0.001$), a longer length of the PFO tunnel (13.4 ± 4.4

vs. 7.8 ± 2.5 , $P<0.001$), a lower IVC-PFO angle (16.4 ± 3.4 vs. 20.3 ± 7.7 , $P=0.001$), a higher proportion of LA multiple exits of the tunnel (46.9% vs. 14.3%, $P<0.001$). Multivariate regression analysis showed that male gender (HR: 4.026, 95% CI: 0.883~18.361, $P=0.072$), age (HR: 1.076, 95% CI: 1.002~1.155, $P=0.045$), the left funnelform (HR:7.299, 95% CI: 1.585~33.618, $P=0.011$), a longer length of the PFO tunnel (HR: 1.843, 95% CI: 1.404~2.418, $P<0.001$) and multiple exits of the tunnel of LA (HR: 8.544, 95%CI: 1.595~45.754, $P=0.012$) increased the risk of cerebral infarction. The cut-off value calculated by ROC for the diagnosis of high-risk PFO was that the length of the PFO tunnel was 12 mm and Left funnelform combined with multiple exits of left atrial (sensitivity was 92%, specificity was 90%). The area under the curve of combine index VS PoPE score (0.932 VS 0.736) relative to the RoPE score was statistically significant.

Conclusions:

A larger oval fossa can be more easily activated and cause a large right-to-left shunt. The left funnelform, a longer length of the PFO tunnel, and multiple exits of the tunnel of LA increase the risk of CS in anatomical of PFO respect. TEE can precisely visualize the specific morphological characteristics of PFO. These features on TEE have a strong correlation with CS.

Keywords: Cryptogenic stroke, Migraine contrast-TEE, Patent foramen ovale, Real-time 3D TEE

Introduction

Patent foramen ovale (PFO) is present in approximately 25% to 30% of the general population [1]. PFO can be found in 27.3% of all adults and is associated with many pathological conditions, such as ischemic stroke, paradoxical embolism, embolic stroke of undetermined source (ESUS), migraine, cerebrovascular injury, non-cerebral paradoxical systemic embolic events, decompression illness, and obstructive sleep apneas [2, 3] [4]. PFO is a potential space or separation between the septum primum and septum secundum in the anterosuperior portion of the atrial septum [5]. The foramen remains functionally closed as long as the LA pressure is greater than the RA pressure. In many cases, a PFO is only functionally patent and has a tunnel-like appearance, as the septum primum forms a flap valve [6](Figure 1). Since PFO is a highly dynamic and complex structure, more studies are needed to confirm the presence of PFO and to rule out pulmonary shunt via intrapulmonary arteriovenous malformations (AVMs). Three-dimensional transesophageal echocardiogram (TEE) is the standard imaging technique for confirming the presence or absence of PFO [7]. Previous studies have shown that the size, length, and width (functional potential) of PFO play a critical role in the development of migraine and ischemic stroke. Additionally, the presence of atrial septal aneurysm (ASA), hypermobile IAS, large RL shunt, Eustachian valve or a Chiari's network, and a sharp ([?]10*) angle between the inferior vena cava and the PFO flap are associated with a high-risk PFO [6, 8-11].

However, previous studies used 2-dimensional imaging of TEE. Most recently, 3D TEE has been described to improve the visualization of PFO, its surrounding tissue rims, and surrounding structures. 3D TEE can be used to guide percutaneous transcatheter closure of PFO [12]. Using 3D TEE, this study compared the

anatomical and functional characteristics of PFO between patients with CS and those without CS to identify high-risk PFO.

Methods:

Study population

In total, 134 consecutive patients with cryptogenic stroke or migraine who had suspected PFO and underwent c-TCD, TTE and TEE at our institution from 5.1.2023 to 3.1.2024 were enrolled in this study (Supplementary Figure). These patients underwent transcatheter closure. All patients provided written informed consent. The study was approved by the Ethics Committee of The Affiliated Hospital of Soochow University (No.235/2024). This study was conducted following the Declaration of Helsinki (as revised in 2013).

The diagnosis of CS was established when patients exhibited a transient or enduring neurological deficit and presented evidence of ischemic lesions on cerebral MRI or CT scans, without an exact explanation of the etiology. The diagnosis of migraine followed the criteria of the International Headache Society [13]. The classification of right-to-left shunt (RLS) severity was as follows: the absence of bubbles was designated as grade 0, the presence of 1-10 bubbles as grade I or mild, 10-30 bubbles as grade II or moderate, and over 30 bubbles as grade III or severe [14].

Contrast -TEE:

The saline contrast consisted of 1 mL air, 1 mL blood, and 8 mL saline. Blood sample was taken using 20-gauge cannulas via the antecubital vein because of its enhanced contrast appearance [15]. The content was agitated between two 10-mL syringes connected with a three-way stopcock and was injected quickly from the anterior cubital vein.

Abdominal compression Valsalva maneuver:

The examiner placed a hand on the patient's right upper abdomen. At this time, the patient was in a state of abdominal relaxation. The examiner pressed the patient's right upper abdominal wall simultaneously with a spontaneous Valsalva maneuver. And check the patient's abdominal muscle contraction. Next, the agitated saline contrast was injected during the Valsalva maneuver phase. Abdominal compression and the Valsalva maneuver were released immediately after the opacification of the right atrium.

PFO confirmation and relevant measurements:

The presence or absence of PFO was confirmed by TEE and cardiac catheterization. TEE (Philips 7c with an X8-2t probe) was performed under local anesthesia. PFO was evaluated at the end of routine examinations. Images of the interatrial septum were obtained from the optimal imaging plane displayed by septal membrane visualization, typically 60 to 90. The excited saline contrast was injected during the strain phase of the Valsalva maneuver. The Valsalva maneuver was released immediately after the opacification of the right atrium. If the left side of the atrial septum was observed, the Valsalva maneuver was considered effective.

The thickness of the primary septum and the secondary septum of PFO was measured at a significantly separated perspective (Figure 2). The height of PFO was regarded as the maximum distance between the primary septum and the secondary septum, and the tunnel length of PFO was regarded as the maximum overlap surface between the primary septum and the secondary septum (Figure 3). Right funnelform shape: the primary septum and secondary septum at the tunnel exit were not obviously separated. The primary septum and the secondary septum at the entrance were obviously separated (Figure 4). The left funnelform was opposite to the right funnel form (Figure 4). Three-dimensional imaging of TEE. The red arrow points to the exit of the PFO tunnel, single channel exit (Figure 5A), more than one channel exit (Figure 5B). Measurement of the fossa oval in 3D-TEE (Figure 6). The presence of PFO was confirmed by actual visualization of microbubbles passing through the compartment, which was achieved by the separation

between the septum primum and septum secundum (Figure 7). We measured the angle between IVC and the PFO valve on the imaging plane, showing the IVC and the atrial septum (Figure 8).

TEE

TEE evaluates atrial septum at a 0 multi-plane angle, in 15 increments. Color Doppler at a low color Doppler scale can help identify flow through the PFO and visualize additional defects in the atrial septum. To capture low-speed blood flow across a small PFO, the color Doppler scale can be slightly reduced to approximately 35-40 cm/sec.

Starting at 30-50 plane angle, the PFO was visualized adjacent to the aorta. Rotation of the imaging plane in 15 increments should line the imaging plane with the pathway or tunnel of the PFO. The length of the PFO tunnel can be assessed from this point of view. The thickness of the septum secundum can also be evaluated from this view. With the visualization of PFO, agitated saline contrast is injected to evaluate right-to-left shunting.

RoPE score

	Points
Patient characteristics	
No history of hypertension	+1
No history of diabetes	+1
No history of stroke or TIA	+1
Non-smoker	+1
Cortical infarct on imaging	+1
Age (years)	
18-29	+5
30-39	+4
40-49	+3
50-59	+2
60-69	+1?;?
70	0

Statistical analysis:

Continuous variables are presented as mean \pm SD or median (interquartile range). Categorical variables are presented as percentages. The t-test was used for normally distributed data, the Mann-Whitney U test was used for non-normally distributed data, and the χ^2 -test was used for categorical variables. Multivariate logistic regression analyses were conducted to assess the anatomical characteristics of the PFO concerning the incidence rate of CS. Odds ratios are reported with 95% confidence intervals. Independent risk factors for CS were determined based on the results of multivariate analysis. Receiver operating characteristic (ROC) curves and area under the ROC curves (AUC) were studied and calculated. For each participant, demographic data and clinical data were analyzed using SPSS 27.0 software, with statistical significance defined as $P < 0.05$.

Results:

1. Study cohort

This study was an observational study. In total, 134 patients were included (male patients $n=55$, 40.7%), with an average age of years (38 ± 11.2) (Table 1). There were 50 patients with severe RLS (right-to-left shunts) and 84 patients with mild-to-moderate RLS (right-to-left shunts). In the massive shunt group, cerebral infarction accounted for 39.6% and migraine accounted for 64%.

2. Severe RLS vs. mild-to-moderate RLS

There was no significant difference in terms of gender (42% vs. 38.8%, $p=0.383$), age (39.76 ± 11.38 vs. 37.98 ± 11.10 , $p=0.373$), previous hypertension (18% vs. 14.1%, $p=0.625$), diabetes (6% vs. 2.4%, $p=0.359$), smoking (16% vs. 15.3%, $p=1.000$), the incidence of cerebral infarction (39.6 vs. 38.5, $p=1.000$), migraine (64% vs. 63.5%, $p=1.000$), the presence of the Eustachian valve or a Chiari's network (10% vs. 5.9%, $p=0.499$), left funnellform (28% vs. 31.8% $p=0.701$), right funnellform (26.0% vs. 21.2%, $p=0.532$), the length of the tunnel (10.2 ± 3.7 vs. 9.7 ± 4.6 , $P=0.585$), the thickness of the primary septum and the secondary septum (1.2 ± 0.3 vs. 1.3 ± 0.4 , 3.7 ± 1.0 vs. 3.5 ± 1.0 , $P=0.172$, $P=0.369$), and the RoPE score and the multiple exits of the tunnel of LA (6.6 ± 1.5 vs. 6.8 ± 1.7 , 28% vs. 27.1%, $P=0.463$, $P=1.000$). However the long diameter of FO (1.74 ± 0.3 vs. 1.60 ± 0.4 , $P=0.039$), short diameter of FO (1.12 ± 0.3 vs. 1.00 ± 0.3 , $P=0.036$), perimeter of FO (4.62 ± 0.7 vs. 4.22 ± 1.0 , $P=0.026$) and area (1.80 ± 0.8 vs. 1.35 ± 0.8 , $P=0.05$) of FO were significantly larger in the severe RLS group.

There were 49 cases of cerebral infarction, 69 cases of migraine, and 16 cases of dizziness. In table 2, compared with the migraine group, the cerebral infarction group had a higher proportion of male participants (59.2% vs. 30.25%, $p=0.002$), a higher age (41.9 ± 8.6 vs. 36.8 ± 12.1 , $P=0.01$), a larger proportion of hypertension (26.5% vs. 9.3% $P=0.012$), a larger number of smokers (30.6% vs. 3.0%, $P<0.001$), a larger proportion of Eustachian valve or a Chiari's network (14.3% vs. 3.5%, $P=0.036$), a larger proportion of left funnellform (55.1% vs. 16.3%, $P<0.001$), a longer length of the tunnel (13.4 ± 4.4 vs. 7.8 ± 2.5 , $P<0.001$), a smaller angle (16.4 ± 3.4 vs. 20.3 ± 7.7 , $P=0.001$), a higher proportion of vascular stenosis in the brain and neck (8.2% vs. 0%, 53.1% vs. 20.9%, $P=0.016$, $P=0.001$), a higher RoPE score (7.6 ± 1.1 vs. 6.3 ± 1.4 , $P<0.001$), and a higher proportion of multiple exits of the tunnel of LA (46.9% vs. 14.3%, $P<0.001$). However, there was no significant difference in shunt between the two groups (36.7% vs. 37.6, $P=0.969$).

3.Multivariate regression analysis showed that male (HR:4.026,95%CI:0.883~18.361, $P=0.072$), age (HR:1.076,95%CI:1.002~1.155, $P=0.045$), left funnellform (HR:7.299, 95%CI:1.585~33.618, $P=0.011$), long tunnel (HR:1.843, 95% CI: 1.404~2.418, $P<0.001$) and multiple exits of the tunnel of LA (HR: 8.544, 95% CI: 1.595~45.754, $P=0.012$) were positively associated with the risk of cerebral infarction (Table 3).

4.The diagnostic performance of high-risk PFO was assessed by using receiver operating characteristic (ROC) curves and the area under the ROC curve analysis show in figure 9 and figure10. The cut-off value calculated by ROC for the diagnosis of high-risk PFO was that the length of the PFO tunnel was 10.4 mm (sensitivity was 90%, specificity was 87%). Left funnellform combined with multiple exits of left atrial (sensitivity was 89%, specificity was 91%). The area under the curve of PFO tunnel length VS left funnellform + multiple exits of left atrial VS PoPE score (0.921 VS 0.932 VS 0.736) relative to the RoPE score was statistically significant. The cut-off value calculated by ROC for the diagnosis of high-risk PFO was that the length of the PFO tunnel was 12 mm and Left funnellform combined with multiple exits of left atrial (sensitivity was 92%, specificity was 90%). The area under the curve of combine index VS PoPE score (0.932 VS 0.736) relative to the RoPE score was statistically significant.

Discussions:

PFO can serve as a conduit for paradoxical embolism, allowing venous thrombi to enter the arterial circulation, avoiding filtration by the lungs, and causing ischemic stroke. The anatomical structure of PFO indicates that in addition to thrombi, it allows harmful circulatory factors to circulate directly from veins to arteries [4]. There are many theories about the mechanism of stroke in patients with PFO: 1) Abnormal embolism, one type of venous thrombosis (also known as air, fat, and infectious substances) enters the arterial circulation through the PFO, avoiding the filtration of the lungs and leading to cerebral embolism; and 2) due to various high-risk anatomical features, primary thrombosis occurs in the PFO lumen.

PFO itself has been suspected as the site of thrombus formation [2, 16]. Consistent with previous studies, this study found that the proportion of PFO long tunnel and the left funnellform was higher in CS.

The potential mechanisms underlying the link between PFO and migraine [17] micro embolus-induced cortical spreading depression (CSD)[18], the vasoactive substance hypothesis [19] and shared genetic predisposition [20]. Migraine is a common and recurrent disease, often confined to one side, manifested as paroxysmal

pain. The symptoms of migraine often include nausea, vomiting, dizziness, photophobia and phonophobia [21]. Studies have shown that migraine can lead to various neurological diseases, including stroke, cerebral infarction, and long-term ischemia-reperfusion injury. Therefore, migraine is considered to be the third most frequent chronic disabling disease worldwide [22]. PFO-related right-to-left shunting allows potentially vasoactive substances to bypass the lung, which may aggravate cerebral injury [23]. 5-HT has been linked to the pathogenesis of migraine [24]. This study found that severe right-to-left shunt was relatively common among patients with severe migraine and stroke. PFO and migraine are both prevalent and have highly heterogeneous presentations. Their coincidence remains a debating issue, but it is less likely a coincidental finding, since experimental micro-embolism can depress cortical spreading [25].

C-TCD diagnosis of RLS mainly relies on the Valsalva maneuver. It is not possible to stimulate right-to-left shunting using Faraday’s maneuver under TEE; thus, we used abdominal compression to stimulate right-to-left shunting. Our findings were highly consistent with the results of the C-TCD stimulation test. The blood flow returning from the vena cava to the right atrium increases and RAP instantly increases after the release of abdominal pressure. When the right atrial pressure increases and exceeds the left atrial pressure, PFO may re-open, and microbubbles can be observed to enter the left atrium through the PFO tunnel.

PFO is a dynamic and three-dimensional structure as it originates from the embryonic septum primum and secundum. The structure of PFO is best described as a dynamic tunnel (not just a “hole”) outlined by opposing myocardial flaps remaining from the fetal septum primum and secundum, which never fully fused to wall off the right atrium from the left atrium. Since the IAS is a complex, dynamic, and 3D anatomic structure, 2D echocardiography cannot comprehensively evaluate it.

Current treatments of PFO include medical treatment utilizing anticoagulants and/or antiplatelet agents, endovascular PFO closure by meshed devices, or even surgical closure. Even “asymptomatic” PFO leads to pulmonary gas exchange inefficiency. Endovascular PFO closure improves exercise capacity and reduces exercise-induced hypoxemia. In clinical settings, patients frequently report improved general exercise tolerance and better vascular perfusion to the extremities after the closure of PFO.

Conclusion

Even if a quarter of people have PFO, or asymptomatic PFO, but prone to right to left PFO there is a risk of unexplained stroke. PFO with high-risk features may lead to clinically significant and clinically asymptomatic events. The evaluation of PFO dynamics using three-dimensional combined two-dimensional echocardiography can help better identify high-risk PFO.

Limitation:

Our study had some limitations as follows:

1. This was a single-center study.
2. Neurologically asymptomatic subjects who have a PFO on TEE would be the ideal participants for the control or comparison group, but for this study, we used patients with migraine as the control group.
3. The grade of RLS might be underestimated because it depends on the degree of Valsalva maneuver.

Author contribution:

Li Wang: Data collation and analysis, methodology, writing the first draft

Haibo Sun: Data collation and analysis

Han Shen: Project management, methodology, monitoring, writing, and editing. All authors studied and approved the final manuscript.

Funding:

This study was specifically funded by The Bo Xi Youth Natural Science Foundation (NO.BXQN2023016)

Acknowledgments:

We would like to thank all patients and researchers involved in this study.

Conflict of interest

None

Competing interests

The authors have no known competing financial interests or personal relationships that could affect the work reported in this paper.

Ethics approval

The Ethics Committee of The Affiliated Hospital of Soochow University (No.235/2024) approved the protocol of this study.

Availability of data and materials

The research data is confidential.

References:

1. Hagen PT, Scholz DG, Edwards WD: **Incidence and size of patent foramen ovale during the first 10 decades of life: an autopsy study of 965 normal hearts** . *Mayo Clin Proc* 1984, **59** (1):17-20.2. Elgendy AY, Saver JL, Amin Z, Boudoulas KD, Carroll JD, Elgendy IY, Grunwald IQ, Gertz ZM, Hijazi ZM, Horlick EM *et al* :**Proposal for Updated Nomenclature and Classification of Potential Causative Mechanism in Patent Foramen Ovale-Associated Stroke** . *JAMA Neurol* 2020, **77** (7):878-886.3. Lammers A, Hager A, Eicken A, Lange R, Hauser M, Hess J: **Need for closure of secundum atrial septal defect in infancy** . *J Thorac Cardiovasc Surg* 2005, **129** (6):1353-1357.4. Ning M, Lo EH, Ning PC, Xu SY, McMullin D, Demirjian Z, Inglessis I, Dec GW, Palacios I, Buonanno FS:**The brain's heart - therapeutic opportunities for patent foramen ovale (PFO) and neurovascular disease** . *Pharmacol Ther* 2013,**139** (2):111-123.5. Calvert PA, Rana BS, Kydd AC, Shapiro LM:**Patent foramen ovale: anatomy, outcomes, and closure** . *Nat Rev Cardiol* 2011, **8** (3):148-160.6. Silvestry FE, Cohen MS, Armsby LB, Burkule NJ, Fleishman CE, Hijazi ZM, Lang RM, Rome JJ, Wang Y: **Guidelines for the Echocardiographic Assessment of Atrial Septal Defect and Patent Foramen Ovale: From the American Society of Echocardiography and Society for Cardiac Angiography and Interventions** .*J Am Soc Echocardiogr* 2015, **28** (8):910-958.7. Schneider B, Zienkiewicz T, Jansen V, Hofmann T, Noltenius H, Meinertz T:**Diagnosis of patent foramen ovale by transesophageal echocardiography and correlation with autopsy findings** . *Am J Cardiol* 1996, **77** (14):1202-1209.8. Nakayama R, Takaya Y, Akagi T, Watanabe N, Ikeda M, Nakagawa K, Toh N, Ito H: **Identification of High-Risk Patent Foramen Ovale Associated With Cryptogenic Stroke: Development of a Scoring System** . *J Am Soc Echocardiogr* 2019,**32** (7):811-816.9. Lucà F, Pino PG, Parrini I, Di Fusco SA, Ceravolo R, Madeo A, Leone A, La Mair M, Benedetto FA, Riccio C *et al* : **Patent Foramen Ovale and Cryptogenic Stroke: Integrated Management** . *J Clin Med* 2023, **12** (5).10. Pu H, Zhang Q, Wu J, Zhang Y, Zhao Y, Li L: **Assessment of the Characteristics of Patent Foramen Ovale Associated with Cryptogenic Stroke** . *Curr Med Imaging* 2024.11. Akagi T: **Transcatheter closure of patent foramen ovale: Current evidence and future perspectives** . *J Cardiol* 2021, **77** (1):3-9.12. Pushparajah K, Miller OI, Simpson JM: **3D echocardiography of the atrial septum: anatomical features and landmarks for the echocardiographer** . *JACC Cardiovasc Imaging* 2010, **3** (9):981-984.13. **The International Classification of Headache Disorders: 2nd edition** . *Cephalalgia* 2004, **24** Suppl 1 :9-160.14. Bernard S, Churchill TW, Namasivayam M, Bertrand PB: **Agitated Saline Contrast Echocardiography in the Identification of Intra- and Extracardiac Shunts: Connecting the Dots** .*J Am Soc Echocardiogr* 2020.15. Fan S, Nagai T, Luo H, Atar S, Naqvi T, Birnbaum Y, Lee S, Siegel RJ: **Superiority of the combination of blood and agitated saline for routine contrast enhancement** . *J Am Soc Echocardiogr* 1999,**12** (2):94-98.16. Yan C, Li H: **Preliminary Investigation of In situ Thrombus Within Patent**

Foramen Ovale in Patients With and Without Stroke . *Jama* 2021, **325** (20):2116-2118.17. Cao W, Shen Y, Zhong J, Chen Z, Wang N, Yang J: **The Patent Foramen Ovale and Migraine: Associated Mechanisms and Perspectives from MRI Evidence** . *Brain Sci* 2022, **12** (7).18. Ashina M, Hansen JM, Do TP, Melo-Carrillo A, Burstein R, Moskowitz MA: **Migraine and the trigeminovascular system-40 years and counting** . *Lancet Neurol* 2019, **18** (8):795-804.19. Wilmshurst P, Nightingale S:**The role of cardiac and pulmonary pathology in migraine: a hypothesis** . *Headache* 2006, **46** (3):429-434.20. Wilmshurst PT, Pearson MJ, Nightingale S, Walsh KP, Morrison WL:**Inheritance of persistent foramen ovale and atrial septal defects and the relation to familial migraine with aura** . *Heart* 2004, **90** (11):1315-1320.21. Ashina M, Terwindt GM, Al-Karagholi MA, de Boer I, Lee MJ, Hay DL, Schulte LH, Hadjikhani N, Sinclair AJ, Ashina H *et al* : **Migraine: disease characterisation, biomarkers, and precision medicine** . *Lancet* 2021,**397** (10283):1496-1504.22. Burch R: **Preventive Migraine Treatment** . *Continuum (Minneap Minn)* 2021,**27** (3):613-632.23. **International Stroke Conference Oral Presentations** . *Stroke* 2011, **42** (3):e42-e110.24. Anthony M, Hinterberger H, Lance JW: **Plasma serotonin in migraine and stress** . *Arch Neurol* 1967, **16** (5):544-552.25. Tietjen GE, Collins SA: **Hypercoagulability and Migraine** . *Headache* 2018, **58** (1):173-183.

Table 1: The characteristics of patients and PFO.

Note: Values are presented as mean±SD or n (%).

Abbreviation: PFO, patent foramen ovale. RoPe, risk of paradoxical embolism. BMI, body mass index. FO, fossa ovale. RLS, right-to-left shunts. LA, left atrium.

Table 2: Comparison of basic characteristics and echocardiographic features between the cryptogenic group and the migraine group.

Note: Values are mean±SD or n (%).

Abbreviation: PFO, patent foramen ovale. RoPe, risk of paradoxical embolism. BMI, body mass index. FO, fossa ovale. RLS, right-to-left shunts. LA, left atrium. TCD, transcranial doppler. IVC, inferior vena cava.

Table 3: Multivariate logistic regression analysis for the echocardiographic characteristics of the cryptogenic group and the migraine group.

Note:

Abbreviation: PFO, patent foramen ovale. LA, left atrium.

Figure 1: Fossa Ovalis and PFO.

Figure 2: The thickness of the primary septum and the thickness of the secondary septum.

Figure 3: The height and length of the PFO tunnel.

Figure 4: Left funnellform and right funnellform.

Figure 5: The exit of the PFO tunnel by three-dimensional TEE.

Figure 6: Measurement of the oval fossa.

Figure 7: The presence of PFO was confirmed by actual visualization of microbubbles passing through the separation between the septum primum and septum secundum.

Figure 8: Measurement of IVC-PFO angle.

Figure 9. The diagnostic performance of high-risk PFO was assessed by using receiver operating characteristic (ROC) curves

Figure 10. The combine index diagnostic performance of high-risk PFO was assessed by using receiver operating characteristic (ROC) curves

Supplementary Figure: Trial flowchart.

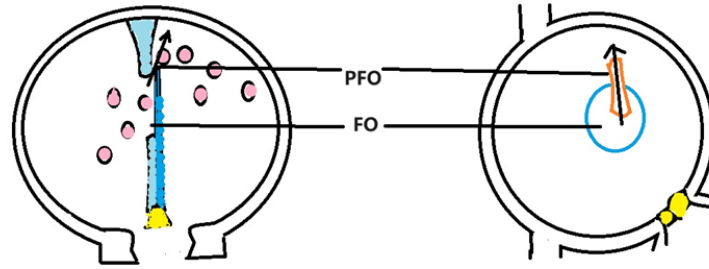


Figure 1 At the anterior superior edge of the fossa ovalis, the primum and secundum septa remain separation, which constitutes a PFO. Arrow denotes blood flowing through the PFO from the embryonic RA to the LA. The blue and the pink dots represent the development of the caval and pulmonary venous inflow to the atria. FO, fossa ovalis. PFO, Patent Foramen Ovale.

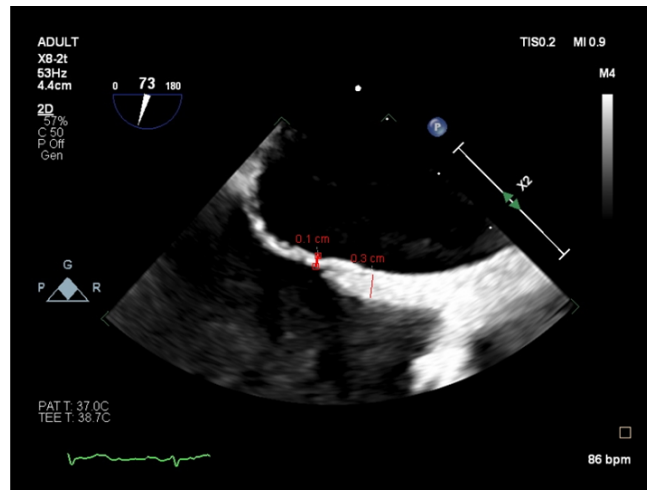


Figure 2, The measurement of the thickness of the primary septum and the thickness of the secondary septum, the red line is expressed as a two-dimensional linear measurement.

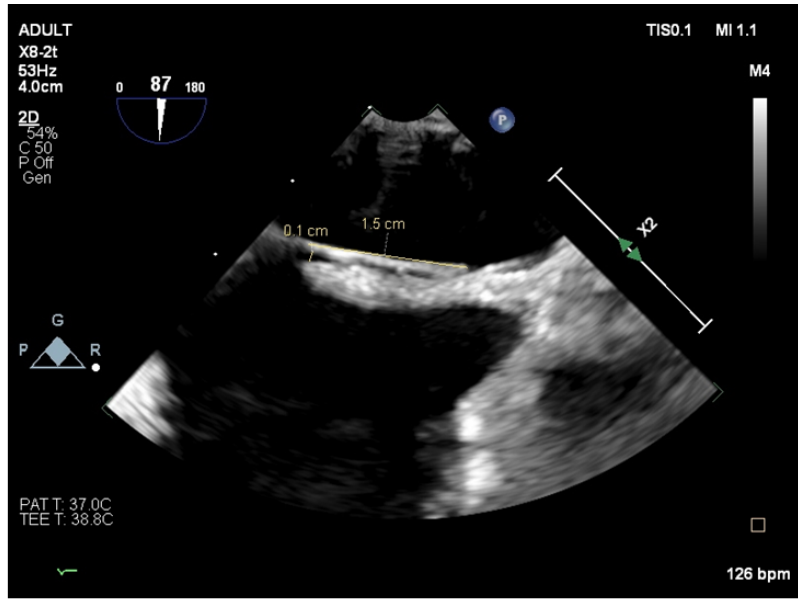


Figure3, The height and length of the Patent Foramen Ovale tunnel, and the yellow line is a two-dimensional measurement.

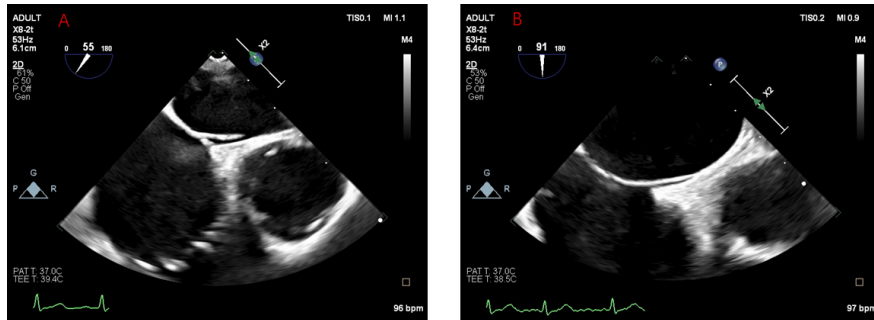


Figure 4 A, Left funnelform, B, Right funnelform

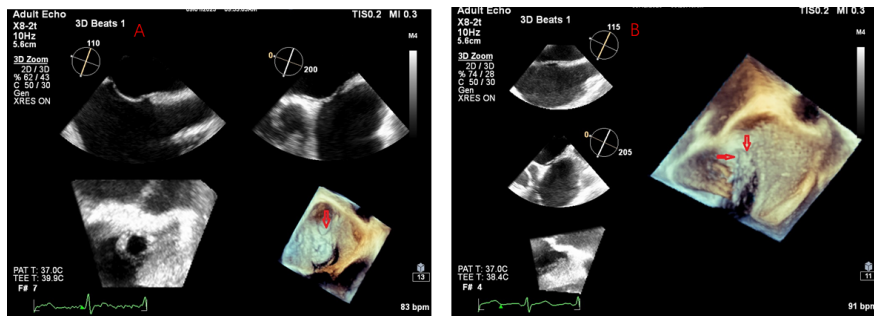


Figure 5, Three -dimensional imaging of transesophageal echocardiography. The red arrow points to the exit of the Patent Foramen Ovale tunnel, A, single channel exit ,B, more than one channel exit.

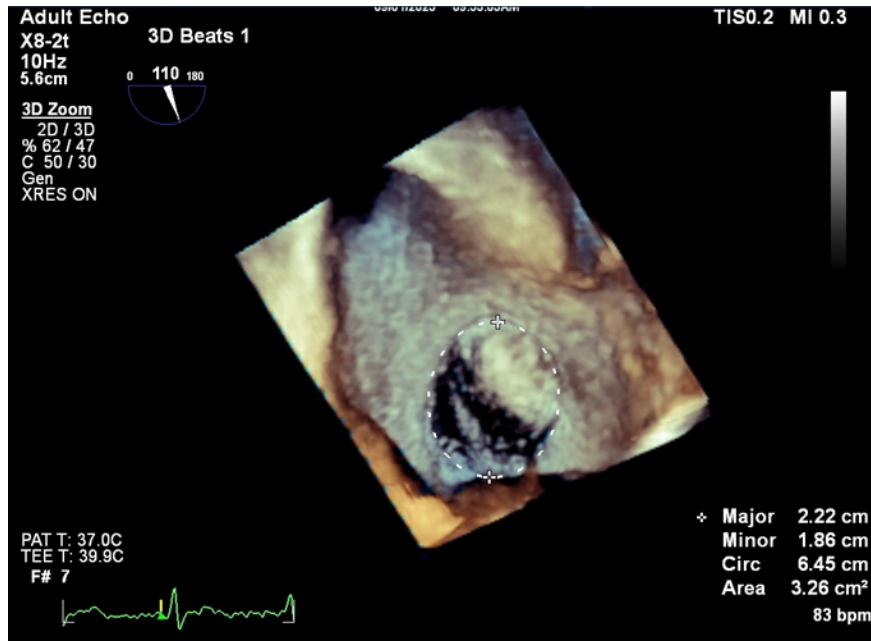


Figure 6 , Measurement of the fossa oval

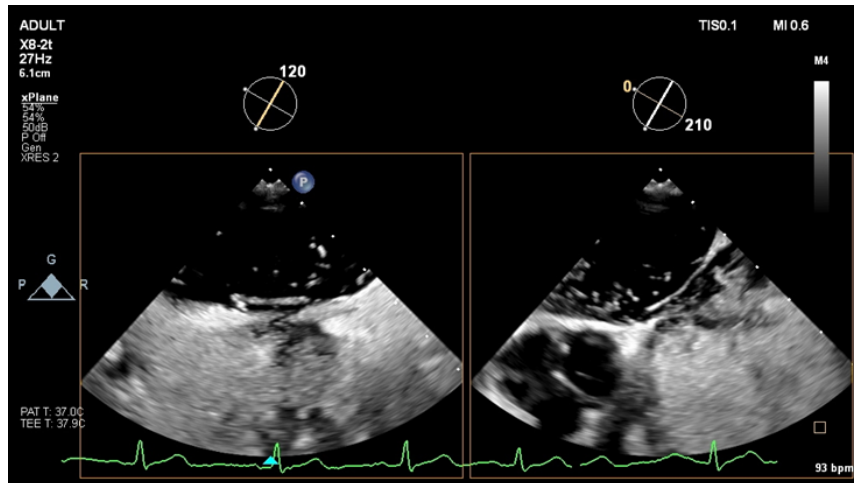


Figure 7, The presence of PFO was confirmed by actual visualization of microbubbles passing through the separation between the septum primum and septum secundum.

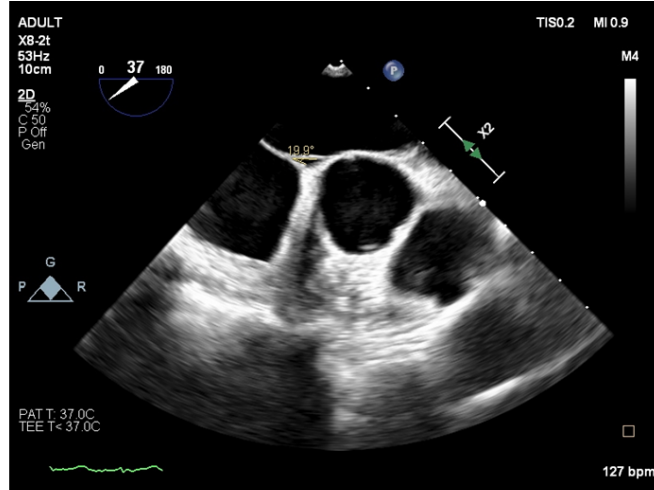


Figure 8, Measurement of IVC-PFO angle, IVC, inferior vena cava, PFO, Patent Foramen Ovale.

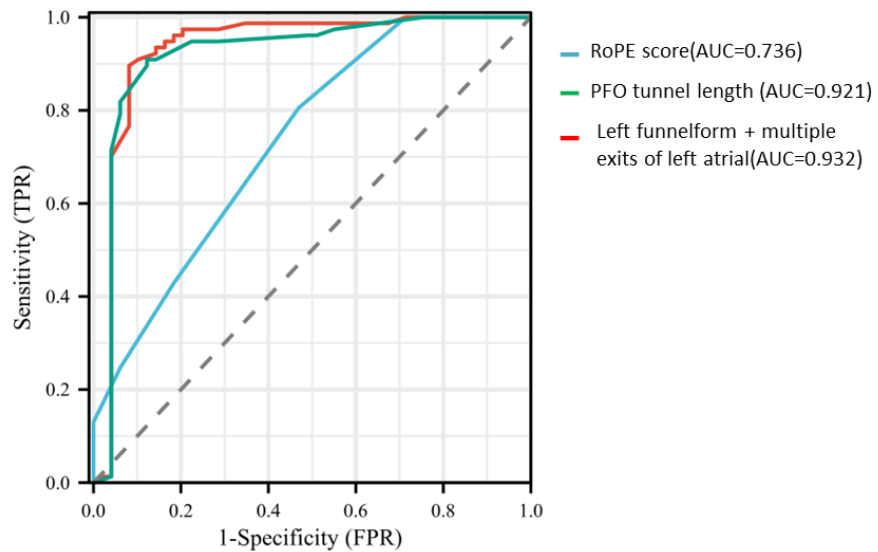


Figure 9. The diagnostic performance of high-risk PFO was assessed by using receiver operating characteristic (ROC) curves

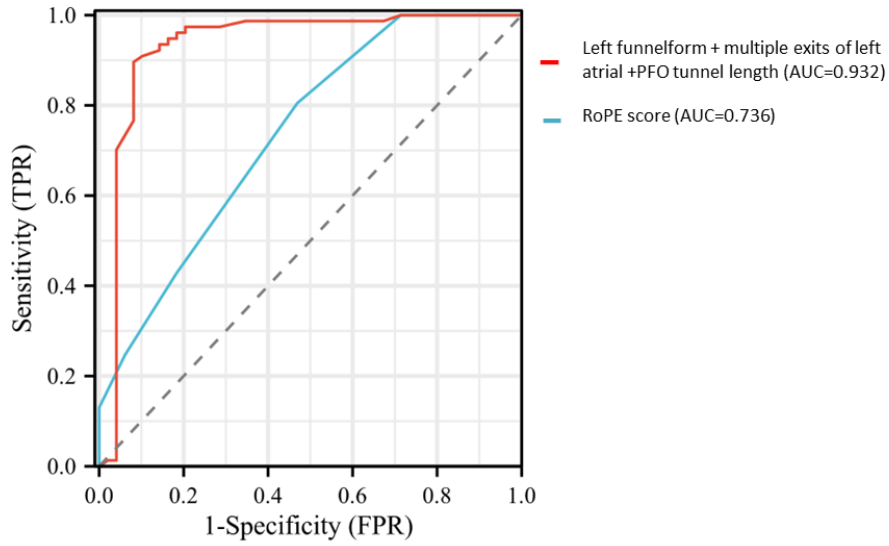
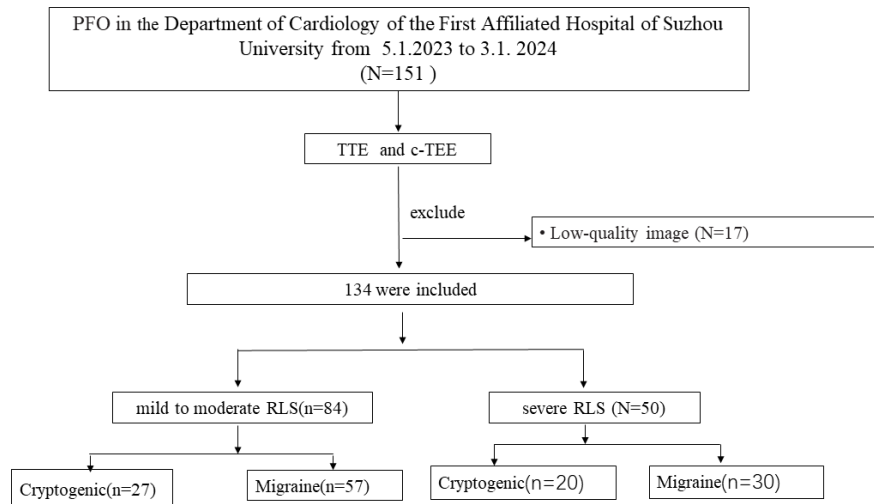


Figure 10. The diagnostic performance of high-risk PFO was assessed by using receiver operating characteristic (ROC) curves



Supplementary Figure : Trial Flow Chart; PFO: Patent Foramen Ovale ; TTE: transthoracic echocardiography; c-TEE: contrast transesophageal. RLS :right to left shunt.

Hosted file

table.docx available at <https://authorea.com/users/733404/articles/1221775-the-anatomical-significance-of-the-patent-foramen-ovale-by-real-time-3d-tee-in-cryptogenic-stroke-and-migraine>